

# A Diffusion-Reaction Model for Integrin Clustering in Response to Cell Adhesion

*Erik S. Welf, Ulhas P. Naik, and Babatunde A. Ogunnaike*

## Introduction

Integrins are plasma membrane proteins that receive signals from inside the cell to anchor the cell to the extra-cellular environment, and relay information about the environment back into the cell. A variety of integrin-dependent pathologies have been identified, including cancer, blood clotting disorders, developmental disorders, heart attack, and stroke<sup>1</sup>. Research has elucidated the form and function of many integrin proteins, but we still do not fully understand how integrins function collectively to relay information bi-directionally through the cell membrane<sup>2</sup>. By forming clusters that anchor cells to the extra-cellular matrix (ECM), integrins provide a platform for signal transduction and cytoskeletal attachment inside cells<sup>3</sup>. The formation of these clusters is a dynamic, spatially heterogeneous process that effects cell growth and movement through various signaling events<sup>4</sup>. However, our understanding of integrin signaling has been limited by our inability to capture the temporal and spatial complexity that is the very basis for integrin clustering and subsequent signaling events. We have developed a mathematical model of integrin movement and clustering that captures different integrin clustering patterns depending on values chosen for certain model parameters. By varying model parameters to reflect integrin behavior, we are able to quantitatively relate collective behavior to specific integrin characteristics.

## Background and Objectives

Upon adhesion, cells have been observed to form clusters of adhesion proteins that differ in their composition, size, and spatial location. The diversity of these clusters then leads to different cytoplasmic signaling events according to the cluster attributes<sup>5</sup>. The formation of these diverse complexes includes the clustering of integrins in the plasma membrane, and the different types of clusters affect intracellular signaling differently. Integrins normally reside diffusely in the cell membrane, with little to no aggregation<sup>6</sup>. This suggests that there must be some biological switch that converts integrins from the dormant, diffuse state, to the activated, clustered state. Though it has been shown that integrin activation for binding to ligand and integrin clustering are separate and distinct events<sup>6</sup>, it has also been shown that both must occur for the formation of integrin clusters that are capable of fostering cell adhesion or migration<sup>5</sup>. The strength of cell adhesion, termed avidity modulation, is determined by the individual integrin bond strength, and the number of integrin bonds<sup>7</sup>. It follows that a certain level of avidity must be reached for the transduction of a critical force that is capable of attaching the cell to the ECM<sup>8</sup>, and this corresponds to both a critical affinity and critical integrin cluster size.

Various research groups have explored how modifications in affinity and avidity affect the size, location, and composition of integrin clusters. Keselowski,

Collard, and Garcia altered integrin binding affinity to ligand and focal adhesion composition by modifying the surface chemistry of Fibronectin (FN), an ECM component to which integrins bind, and they were able to correlate integrin binding affinity with cell adhesion<sup>9</sup>. Kato and Mrksich altered the structure of an integrin binding sequence to create a linear or cyclic structure, and noted alterations in binding affinity and integrin cluster size distribution<sup>10</sup>.

Cells control the size, number, and temporal characteristics of integrin clusters and the subsequent cellular signals by controlling integrin behavior; with this model, key aspects of integrin clustering are recreated by varying model parameters. This gives us the ability to understand how alterations in integrins' specific physical properties, such as binding affinity or activation state, relate to quantitative changes in integrin clustering and cell behavior. Changes in integrin clustering may then be related quantitatively to cell signaling events. *The goal of the model presented here is to describe how changes in integrin properties, such as affinity and avidity, can be associated with key model parameters and thus enable us to characterize the resultant effects upon integrin cluster formation.*

### Model Formulation

In order to cast the model, we assume that integrins are mobile and subject to Fickian diffusion in the free, unbound state, and that they are immobile when bound to an insoluble ECM substrate. In the model, integrin clusters form via two sequential reactions. An initial, reversible reaction creates a loosely bound form that quickly converts to a tightly bound form when the appropriate conditions for integrin clustering are satisfied. Integrin clusters are formed by the association of tightly bound integrins into regions of high concentration of the tightly-bound species.

Integrins, when not bound to the cell cytoskeleton, are free to diffuse throughout the plasma membrane<sup>6</sup>. Un-activated integrins do not bind ligand, and therefore continue to diffuse until they become activated for ligand binding, whereupon adhesion to an insoluble substrate, or attachment to the cell cytoskeleton prevent integrin movement. A conformation change or detachment from an immobile substance upon integrin activation causes integrins to move more freely. Our model represents integrin movement by assuming Fickian diffusion for free, unbound integrin in one spatial dimension. Fickian diffusion implies that molecular species move in a continuous fashion in response to a difference in concentration; the driving force for movement is the concentration gradient, as shown in Equation 1 below.

$$J_A = D_A \nabla C_A \quad (1)$$

The flux  $J_A$  is defined as the species flow per unit area per unit time. Assuming constant fluid density in the absence of convective transport, the flux of species A is equal to the diffusivity for species A,  $D_A$  times the gradient of the concentration of species A. In one dimension ( $x$ ), the flux of species A is given by:

$$J_A = D_A \frac{\partial C_A}{\partial x} \quad (2)$$

Applying a species balance across a control volume yields the following transport equation for species A (in rectangular coordinates).

$$\frac{\partial C_A}{\partial t} + v_x \frac{\partial C_A}{\partial x} + v_y \frac{\partial C_A}{\partial y} + v_z \frac{\partial C_A}{\partial z} = D_A \left[ \frac{\partial^2 C_A}{\partial x^2} + \frac{\partial^2 C_A}{\partial y^2} + \frac{\partial^2 C_A}{\partial z^2} \right] + R_A \quad (3)$$

Here  $R_A$  represents reaction of species A;  $v_x$ ,  $v_y$ , and  $v_z$  represent velocity terms for convective flow, respectively, in the  $x$ ,  $y$ , and  $z$  spatial dimensions. For the purpose of this model, we consider integrins diffusing in one dimension, as they would along the advancing edge of a migrating cell. Reducing this equation to one representing a one-dimensional, non-convective system, we have:

$$\frac{\partial C_A}{\partial t} = D_A \left[ \frac{\partial^2 C_A}{\partial x^2} \right] + R_A \quad (4)$$

We represent integrin function by defining four species: unbound integrin I, ECM ligand L, loosely-bound integrin B, and tightly-bound integrin BT. Unbound integrin converts to bound integrin by reacting reversibly with ligand, and bound integrin converts to tightly-bound integrin through a uni-molecular reaction. This relationship is shown along with the reaction rate constants in the in the expression below.



Reaction fluxes are represented using mass-action kinetics, combined with a stochastic term that creates random positions with high clustering potential. The only mobile species is unbound integrin, and the governing equations are shown below.

$$\frac{\partial C_I}{\partial t} = D_I \left[ \frac{\partial^2 C_I}{\partial x^2} \right] - k_1^f C_I C_L + k_1^r C_B \quad (6)$$

$$\frac{\partial C_L}{\partial t} = -k_1^f C_I C_L + k_1^r C_B \quad (7)$$

$$\frac{\partial C_B}{\partial t} = k_1^f C_I C_L - k_1^r C_B - k_2^f(x) C_B - k_2^s C_B C_{BT} \quad (8)$$

$$\frac{\partial C_{BT}}{\partial t} = k_2^f C_B + k_2^s C_B C_{BT} \quad (9)$$

The reaction of bound integrin to tightly bound integrin is the critical step in integrin cluster formation, because this step forms the high concentration of tightly bound itnegrins that we consider integrin clusters. This second reaction is considered irreversible during the time scale considered, because it constitutes the formation of stable clusters, and we are assuming that stable clusters are not dispersed until an intracellular signal instructing integrin dispersion is received.

Integrins do not form clusters evenly across the surface of a cell. Random events, such initial integrin distribution, cytoskeletal structure, and ECM configuration contribute to spatial variation in the clustering of integrins. In order to incorporate the somewhat random nature of integrin cluster formation, we incorporated a stochastic scaling factor into the rate constant  $k_2^f$ . Since the rate constants  $k_2^f$  and  $k_2^s$  control the conversion of  $B$  to  $BT$ , and the reaction involving  $k_2^s$  requires species  $BT$ , the probabilistic scaling of  $k_2^f$  limits the overall formation of the tightly-bound integrin  $BT$  that forms a stable cluster. The scaling factor for  $k_2^f$  is obtained by assigning a random number from a Guassian distribution to each position along the mesh that is used to solve the PDE's (5)-(8). Since we desire a scaling factor between 0 and 1, the number  $P(x)$  is chosen from a normally-distributed population with mean 0.5 and standard deviation that is controlled to yield the desired variability between sample runs. In order to create separation between high and low random numbers, we pass the random numbers  $P(x)$  through a sigmoid function  $Q(P)$ , shown below. A sigmoid was chosen because it is often nature's way of representing a switching mechanism, and the selection does not imply significance of the function chosen.

$$Q(P) = 1/(1 - \lambda_1 \lambda_2 (\lambda_3 - P)) \quad (10)$$

The parameters  $\lambda_1$ ,  $\lambda_2$ , and  $\lambda_3$  were held constant over all simulations to achieve consistent separation between positive (reaction) events and negative (no reaction) events.

### Model Parameter Analysis

To facilitate model analysis, model equations and independent variables were reduced to dimensionless form, as shown below. Concentrations were normalized by the initial concentration of free integrin,  $C_i$ , which is also the limiting reagent in this reaction scheme. Definitions of the dimensionless variables and parameters are shown in Table 1. The initial conditions used in all simulations (for all  $x$ ) are:  $\varphi = 0.2$ ,  $\psi = 1$ ,  $\eta = 0$ ,  $\zeta = 0$ , thus limiting the reactions by limiting the unbound integrin. Throughout all simulations, the concentrations of all species in dimensionless form fall between 0 and 1.

**Table 1. Model Parameters**

Description	Dimensional Form	Dimensionless Form
Spatial Variable	$x$	$\xi = x \sqrt{\frac{k_1^r}{D_I}}$
Time	$t$	$\tau = tk_1^r$
Free Integrin	$C_I$	$\phi = \frac{C_I}{C_L^o}$
Free ECM	$C_L$	$\psi = \frac{C_L}{C_L^o}$
Bound integrin	$C_B$	$\eta = \frac{C_B}{C_L^o}$
Tightly-bound Integrin	$C_{BT}$	$\varsigma = \frac{C_{BT}}{C_L^o}$
Integrin Affinity for ECM	$k_1^f$	$\Lambda = \frac{k_1^f}{k_1^r} C_L^o$
Nucleation Rate Constant	$k_2^f$	$\Delta = \frac{k_2^f}{k_1^r}$
Cluster Growth Rate Constant	$k_s^f$	$\Gamma = \frac{k_s^f}{k_1^r} C_L^o$

To ensure that the model realistically represents the phenomenon of integrin clustering, we performed an ‘order-of-magnitude’ analysis of the model parameters. Using the relationships between variables and parameters outlined in Table I, we are able to use this analysis to gain confidence in the model’s applicability to this system. Given that we know the diffusion coefficient for integrins,  $D_I$  [m<sup>2</sup>/s] to be  $O(10^{-14})$ <sup>11</sup>, we can use estimates of the values for the time to cluster, and cluster size to obtain estimates for the critical values of the dimensionless parameters that give rise to integrin clustering. By using values for the critical time [s],  $O(10^2)$ , critical diameter [m]  $O(10^{-6})$ , and integrin binding event [s]  $O(10^0)$ , we obtain estimates for the dimensionless parameters,  $\tau_{crit}$  and  $\xi_{crit}$ , that are  $O(10^2)$ , and  $O(10^1)$ , respectively. These estimates agree roughly with the values for  $\tau_{crit}$  and  $\xi_{crit}$ , that result from simulation of the model presented here.

## Results

Through the use of this simple diffusion-reaction framework, we are able to enact changes in integrin cluster number, size and formation time. Analysis of the computational results from this model provides insight into the balance that must be achieved between competing mechanisms for integrin cluster formation.

A simple Analysis of Variance (ANOVA) indicated significant effects resulting from changes to the three main dimensionless parameters,  $\Lambda$ ,  $\Delta$ , and  $\Gamma$ . Changes in  $\Lambda$  and  $\Gamma$  altered the integrin cluster size distributions differently and independently. Changes in all three parameters resulted in changes in the mean time to form integrin clusters. Overall, modest changes to the three main model parameters were able to enact significant, but stable changes in integrin clustering characteristics, as described by this model.

We hypothesized that the time it takes for integrins to reach a critical cluster size could be a rate-limiting step in cell migration and adhesion. Therefore, we investigated the effects of model parameters on integrin clustering time. Individual increases in all three parameters,  $\Lambda$ ,  $\Delta$ , and  $\Gamma$  (all others set at nominal values) decreased the mean cluster time, as expected, due to increases in the rate of reaction of unbound integrins to the tightly bound form. The marginal decreases in mean cluster time lessened as all three parameters reached saturating values, above which the clusters did not form faster. The greatest overall decrease in the cluster time was due to increases in  $\Lambda$ , which corresponds to an increase in the affinity of unbound integrins for ECM. The decrease in cluster time due to increase in  $\Lambda$  is shown in Figure 1.

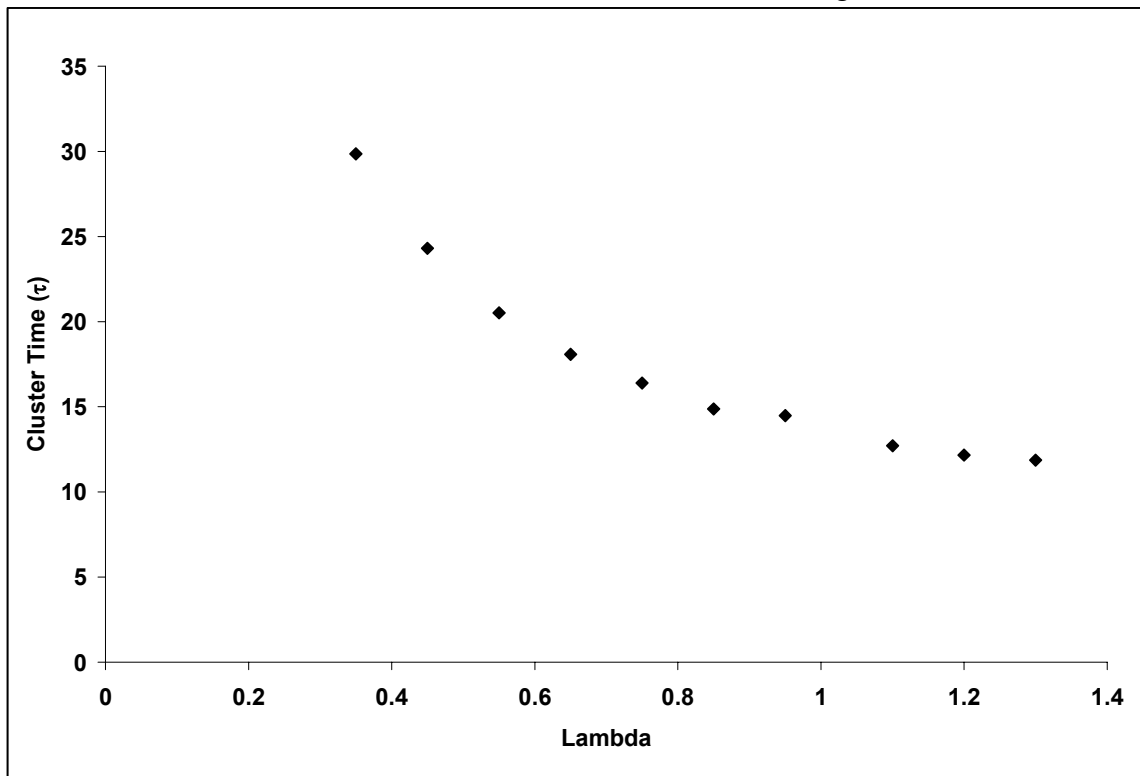


**Figure 1.** Effects of  $\Lambda$  on integrin cluster formation time.

It was of particular interest to investigate the changes in the size distribution of integrin clusters due to changes in model parameters. A value of  $\Lambda$  equal to 0.2 (all other parameters set at nominal values) resulted in a size distribution having a mean near 20 units and a relatively small variance. When  $\Lambda$  was changed incrementally from 0.3 to 1.3 as shown in Figure 2, a second

population appeared with a mean near 35 units.

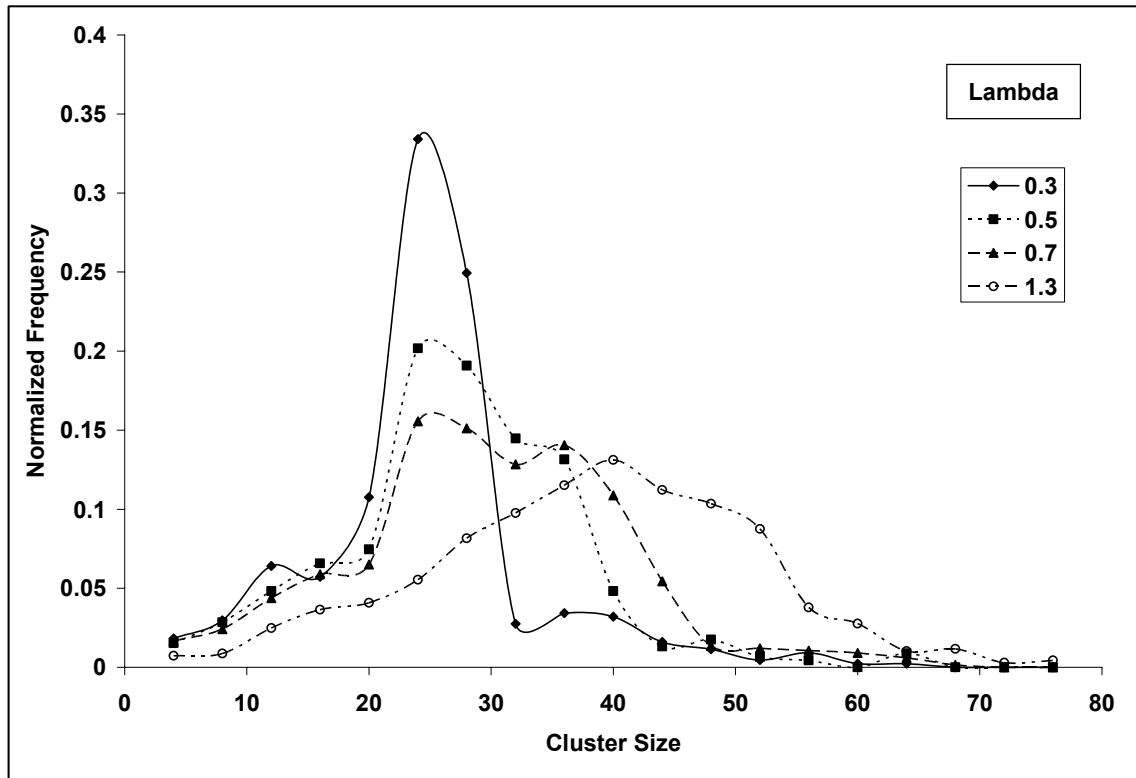


**Figure 2.** Effects of  $\Lambda$  on integrin cluster size distribution.

The second, larger population grew in number at the expense of the smaller population as  $\Lambda$  increased, until the smaller population ceased to appear at all. At the highest levels of  $\Lambda$  tested (1.3), no incremental change in the size distribution was observed, as the population took on a broad, flat distribution with a mean near 40 units. These findings indicate that this simple model framework is capable of representing how changes in integrin affinity for ECM may result in significant changes to the integrin cluster size distribution.

We also investigated the incremental effects of changes in  $\Gamma$ , which is equivalent to the attraction of loosely bound integrins into large tightly bound clusters, on the integrin cluster size distribution. The effects of changes in  $\Gamma$  on the integrin cluster size distribution are shown in Figure 3. At a  $\Gamma$  value of 0.9, the integrin size distribution showed a single peak at approximately 20 units, and increases in  $\Gamma$  smoothly shifted the mean of this peak higher, while broadening the distribution. In contrast to the multiple size distribution populations observed due to changes in  $\Lambda$ , changes in  $\Gamma$  simply shifted the distribution higher while spreading it out across a higher range. Given the theoretical significance of the  $\Gamma$  value, it is not surprising that increases in the propensity for forming large, synergistically-formed clusters increases some clusters greatly, while leaving some clusters smaller because of a lack of free integrins.

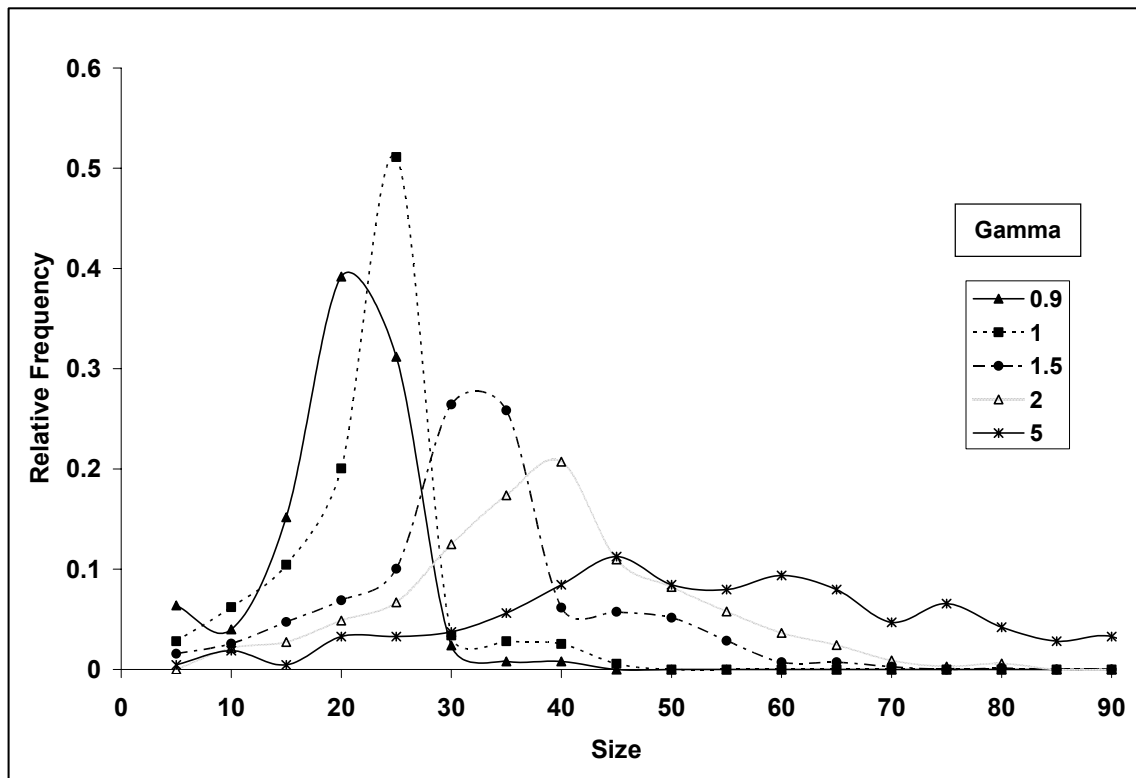


**Figure 3.** Effects of  $\Gamma$  on integrin cluster size distribution.

Overall, we have shown how a simple framework for integrin diffusion and reaction can lead to varied and interesting integrin clustering behaviors due to changes in a few key model parameters. The reaction scheme was based upon the simplest possible mechanisms that explain our current understanding of integrin function, while providing for the alteration of integrin behavior. This gives us the ability to relate model results to actual integrin characteristics, such as binding affinity or activation state. The coupling of this model to various integrin signaling processes, such as migration or apoptosis, will help us to understand how changes in integrin behavior can lead to various integrin-dependent signaling events.

<sup>1</sup> Wehrelle-Haller B, and Imhof BA, *J Pathol* 200, 481-487, 2003.

<sup>2</sup> Calderwood DA, *J Cell Sci* 117, 657-666, 2004.

<sup>3</sup> Clark EA, and Brugge JS, *Science* 268, 233-239, 1995.

<sup>4</sup> Calderwood DA, *J Cell Sci* 117 (5), 657-666, 2004.

<sup>5</sup> Miyamoto S, Teramoto H, Coso OA, Gutkind JS, Burbelo PD, Akiyama SK, and Yamada KM, *J Cell Biol* 131, 791-805, 1995.

<sup>6</sup> Kim M, Carman CV, Yang W, Salas A, and Springer TA, *J Cell Biol* 167, 1241-1253, 2004.

<sup>7</sup> Carman CV, and Springer TA, *Curr Opin Cell Biol*, 15, 547-556, 2003.

<sup>8</sup> Gallant ND, Michael KE, and Garcia AJ, *Mol Biol Cell* 16, 4329-4340, 2005.

<sup>9</sup> Keselowsky BG, Collard DM, and Garcia AJ, *Biomaterials* 25, 5947-5954, 2004.

<sup>10</sup> Kato M, and Mrkish M, *Biochemistry* 43, 2699-2707, 2004.

<sup>11</sup> Yauch RL, Felsenfeld DP, Kraeft S-K, Chen LB, Sheetz MP, and Hemler ME, *J Exp Med* 186, 1347-1355, 1997.